frontiers | Frontiers in Public Health

TYPE Original Research
PUBLISHED 01 December 2022
DOI 10.3389/fpubh.2022.941773

OPEN ACCESS

EDITED BY
Olivier Vandenberg,
Laboratoire Hospitalier Universitaire de Bruxelles (LHUB-ULB), Belgium

REVIEWED BY
Kingsley Eghonghon Ukhurebor,
Edo University, Nigeria
Zisis Kozlakidis,
International Agency for Research on Cancer (IARC), France

*CORRESPONDENCE
Arijit Chakravarty
arijit@fractaltx.com

SPECIALTY SECTION
This article was submitted to Infectious Diseases: Epidemiology and Prevention, a section of the journal Frontiers in Public Health

RECEIVED 11 May 2022
ACCEPTED 04 November 2022
PUBLISHED 01 December 2022

CITATION
Van Egeren D, Stoddard M, Malakar A, Ghosh D, Acharya A, Mainuddin S, Majumdar B, Luo D, Nolan RP, Joseph-McCarthy D, White LF, Hochberg NS, Basu S and Chakravarty A (2022) No magic bullet: Limiting in-school transmission in the face of variable SARS-CoV-2 viral loads. *Front. Public Health* 10:941773. doi: 10.3389/fpubh.2022.941773

No magic bullet: Limiting in-school transmission in the face of variable SARS-CoV-2 viral loads

Debra Van Egeren[1,2], Madison Stoddard[3], Abir Malakar[4,5], Debayan Ghosh[5], Antu Acharya[5], Sk Mainuddin[5], Biswajit Majumdar[5], Deborah Luo[6], Ryan P. Nolan[7], Diane Joseph-McCarthy[8], Laura F. White[9], Natasha S. Hochberg[10,11], Saikat Basu[4] and Arijit Chakravarty[3]*

[1]Department of Medicine, Weill Cornell Medicine, New York, NY, United States, [2]New York Genome Center, New York, NY, United States, [3]Fractal Therapeutics, Cambridge, MA, United States, [4]Department of Mechanical Engineering, South Dakota State University, Brookings, SD, United States, [5]Department of Civil Engineering, Jadavpur University, Kolkata, India, [6]Amity Regional High School, Woodbridge, CT, United States, [7]Halozyme Therapeutics, San Diego, CA, United States, [8]Department of Biomedical Engineering, Boston University, Boston, MA, United States, [9]Department of Biostatistics, Boston University School of Public Health, Boston, MA, United States, [10]Section of Infectious Diseases, Department of Medicine, Boston University School of Medicine, Boston, MA, United States, [11]Department of Epidemiology, Boston University School of Public Health, Boston, MA, United States

In the face of a long-running pandemic, understanding the drivers of ongoing SARS-CoV-2 transmission is crucial for the rational management of COVID-19 disease burden. Keeping schools open has emerged as a vital societal imperative during the pandemic, but in-school transmission of SARS-CoV-2 can contribute to further prolonging the pandemic. In this context, the role of schools in driving SARS-CoV-2 transmission acquires critical importance. Here we model in-school transmission from first principles to investigate the effectiveness of layered mitigation strategies on limiting in-school spread. We examined the effect of masks and air quality (ventilation, filtration and ionizers) on steady-state viral load in classrooms, as well as on the number of particles inhaled by an uninfected person. The effectiveness of these measures in limiting viral transmission was assessed for variants with different levels of mean viral load (ancestral, Delta, Omicron). Our results suggest that a layered mitigation strategy can be used effectively to limit in-school transmission, with certain limitations. First, poorly designed strategies (insufficient ventilation, no masks, staying open under high levels of community transmission) will permit in-school spread even if some level of mitigation is present. Second, for viral variants that are sufficiently contagious, it may be difficult to construct any set of interventions capable of blocking transmission once an infected individual is present, underscoring the importance of other measures. Our findings provide practical recommendations; in particular, the use of a layered mitigation strategy that is designed to limit transmission, with other measures such as frequent surveillance testing and smaller class sizes (such as by offering remote schooling options to those who prefer it) as needed.

KEYWORDS

SARS-CoV-2, epidemiological modeling, schools, environmental controls, viral variants

Introduction

Continued high levels of SARS-CoV-2 transmission strain healthcare systems and accelerate viral evolution, undermining vaccinal efficacy (1, 2) and generating new variants with unpredictable epidemiological characteristics. For example, the transmissibility of SARS-CoV-2 has increased over time, with the Delta variant being around twice as transmissible (3) as the ancestral strain, which had an R_0 (reproduction number) of between 3.3 (4) and 5.7 (5). The incubation time of the disease has also demonstrated evolutionary change, going from 5 to 21 days for the ancestral strain (6, 7) to 2–4 days for the Omicron variant (8).

In order to slow viral evolution by limiting transmission, it is important to understand the role of schools in facilitating SARS-CoV-2 spread. In most countries, a significant fraction of the population consists of K-12 students, staff and first-degree household contacts of students and staff. In the US, 40% of all households have a child at home under 18 years of age (9), and 23% of the US population is enrolled in school (10). Thus, in-school transmission of SARS-CoV-2 will substantially impact transmission dynamics in the whole population.

A number of studies during the early part of the pandemic led to the perception that SARS-CoV-2 did not spread in schools, based on the similarity in case counts between schools and their surrounding communities and a lack of observed transmission chains among children in schools. However, the methodological validity of these conclusions is debatable, as the metrics being used to infer a lack of spread are themselves vulnerable to a "false negative" problem (absence of evidence is not evidence of absence) [see Supplementary material S2, and White et al. (11) for a detailed critique on the limitations of current research arguing that SARS-CoV-2 does not spread in schools]. In fact, there is now a robust body of evidence supporting the contention that SARS-CoV-2 spreads efficiently in schools that lack adequate infection control measures. Empirical analyses using county-level panel data in the United States have demonstrated that counties with fully open K−12 schools with in-person learning had a 5% increase in the growth rate of COVID-19 cases during April–December 2020 (a period of time when US schools were largely closed for the first five months) (12). Consistent with this finding, COVID-19 symptom reporting was more common in areas where schools were open compared to areas with remote learning, an effect that was attenuated in communities using multiple mitigation measures (13). In-school transmission is apparent when systematic surveillance testing methods are used (14–17), and dramatic increases in case detection rates have also been observed in studies that relied on surveillance as opposed to symptomatic testing (18).

A layered mitigation strategy is one way to limit transmission in the school setting under conditions of widespread community transmission. There are multiple potential interventions currently available: vaccines, masks, air quality improvements, surveillance testing, contact tracing/isolation and podding. For reasons of cost and practicality, we seek a minimal set of infection-control measures that can effectively limit in-school spread. However, ongoing viral evolution can yield further changes to the characteristics of the virus, and a set of infection control measures that works well for one viral variant may readily be defeated by the next.

An important open question then is: "What is the design of a minimal set of infection-control measures in schools that is robust to variant-to-variant differences in viral load?" In this work, we used mathematical modeling of the steps involved in viral transmission to understand the impact of infection-control measures in a range of different scenarios corresponding to variants with differing viral loads. Our results address both the feasibility and robustness of strategies for limiting SARS-CoV-2 transmission in schools. We found that a strategy with several different components (masking, ionizers, and air filters) is necessary for reducing viral transmission, particularly for high viral load variants. These control strategies have not been implemented in many US school settings, opening the door to SARS-CoV-2 spread in the classroom and its associated immediate and delayed health consequences for the general population.

Methods

To estimate the risk of viral transmission we built a multistep model comprising emission of viral particles into the air and subsequent inhalation and deposition into the nasopharynx of uninfected individuals (Supplementary Figure S1).

Estimating viral steady-state concentrations in a room with an infected individual

We designed a mathematical model of viral concentrations in a room in which an infected individual emits airborne SARS-CoV-2 particles at a constant rate. We assumed that the airborne virions are distributed uniformly throughout the room (i.e., the air in the room is well-mixed). Virions are inactivated at a constant rate and have an average lifetime of approximately 1.6 h indoors at 73°F, 55% humidity (19). For a closed room with no air exchange or filtration, the change in virion concentration over time is given by the differential equation

$$\frac{dC}{dt} = \frac{\alpha}{V} - \delta C \quad (1)$$

where α is the viral emission rate, δ is the viral inactivation rate, V is the volume of the room, and t is the amount of time elapsed since the infected individual entered the room.

Therefore, the viral concentration in the air over time $C(t)$ is

$$C(t) = \frac{\alpha}{\delta V}(1 - e^{-\delta t}) \quad (2)$$

Air filtration removes virions in the room by filtering out a certain fraction of viruses that pass through the filter. Assuming the room is well-mixed, this adds an additional first-order virus removal process with rate $\varepsilon\beta/V$ where ε is the fraction of virions that are eliminated while passing through the filter (between 0 and 1), β is the rate at which room air is passed through the filter (in units of air exchanges per hour), and V is the room volume. With filtration, the concentration in the air is

$$C(t) = \frac{\alpha}{(\delta + \frac{\varepsilon\beta}{V})V}(1 - e^{-(\delta + \frac{\varepsilon\beta}{V})t}) \quad (3)$$

Ionizers simply increase the virus inactivation rate δ.

For the ancestral virus strain, we estimated the rate at which infected individuals emit viral particles into the air using published data which show that rooms with infected individuals have approximately 2–6 viral copies per L of air (20). Assuming these measurements were taken when the virus was at a steady-state concentration in the room and that these individuals were in a reasonably sized room (4,000 cubic feet of air), we estimated that the viral emission rate would be approximately 2,319–6,937 virions/h using our equation for the viral steady-state contribution shown in the Results. Therefore, we used a value within this range (5,000 virions/h) for the emission rate for the low viral load simulations in this study. See Supplementary material S6 for details about parameter estimates for various interventions.

Estimating the risk of infection based on the steady-state viral concentration in a room

To cause a new infection, virions must be inhaled by an uninfected host and be deposited in the airway mucosa, where they can replicate and cause disease. The rate at which virions are inhaled is the product of the respiratory tidal volume (volume of air inhaled during each breath) and the respiratory rate. However, computational fluid dynamics suggests that a minority of inhaled virions hit the nasopharyngeal mucosa, and this probability depends on the size of the liquid droplets containing the virions (21). We used published estimates of the respiratory droplet size distribution (22) and the probability of hitting the nasopharynx for different inhaled droplet sizes (21) to estimate the overall fraction of inhaled virions that are deposited in the airway mucosa, marginalized over the empirical respiratory droplet size distribution, as

$$\sum_i v_i s_i d_i \quad (4)$$

where s_i is the fraction of exhaled droplets of size i, d_i is the probability of mucosal deposition for droplets of size i, and v_i is the fraction of aerosolized virions that are contained in droplets of size i. This fraction v_i is calculated as

$$v_i = \frac{r_i^3}{\sum_i r_i^3} \quad (5)$$

where r_i is the radius of the droplets of size i. To calculate the time until infection of an uninfected host, we conservatively assumed that 500 virions were required for infection (see Supplementary material S7 for details about the minimum infectious dose).

Numerical simulations of air mixing and exhalation patterns inside a realistic ventilated classroom

Flow physics play a vital role in the distribution of airborne pathogens inside a confined space such as a classroom. To model that, we have implemented state-of-the-art Computational Fluid Dynamics (CFD) simulations of air transport inside the room owing to incoming flux through the open windows and exhaled streamline patterns from human emitters situated at different points of the room. The digital reconstruction of the room is based on the measurements from an auditorium-style classroom. The room was sized at 13 × 8 × 5 m, with three windows (each 1 × 1.25 m) and a door (1 × 2.25 m). A head-sized sphere was used to stand in for the emitter's head in each simulated flow model and was subtracted from the corresponding interior mesh. The sphere has nasal protuberances, bearing nostrils realistically sized at 107.65 and 125.33 mm^2, based on computed tomography reconstructions of human subjects (21). For the emitter's locations, we tested four different scenarios: (i) streamlines emitted by the teacher standing on a podium at the front of the classroom, (ii) a student seated in the front row, (iii) a student seated in the middle of the auditorium, and (iv) a student situated at the rear row. The classroom interior is meshed on ICEM CFD 2019 R3 (ANSYS Inc., Canonsburg, Pennsylvania) with tetrahedral elements bearing a maximum size of 0.15 m. The resolution was based on an earlier study (23) on meshing requirements (maximum size < 0.2 m) to numerically model natural ventilation. Additionally, five layers of prism elements (23) with a height ratio of 1.2 are extruded on the boundary walls. The meshed geometries were then imported to ANSYS Fluent 2019 R3 to track the air transport using the shear-stress transport (SST) k-ω model (24) to account for the turbulent flow scales.

When wind encounters a blocking effect on its path owing to a building, the velocity pressure is converted into static pressure. Consequently, on the windward side, the pressure

would increase, with consequent pressure reduction on the leeward side. The static pressure gradient generated by wind on the building surface can be estimated by:

$$\triangle P_w = \frac{1}{2} C_p \rho_o U^2 \quad (6)$$

where $\triangle P_w$ is the static pressure difference, C_p is the wind pressure coefficient, ρ_o is the density of outside air, and U is the mean wind velocity. The C_p value, which is independent of wind speed but depends upon wind direction and incident angle, can be calculated for low storied buildings (for up to 3 stories) (25). The other physical parameters, namely ρ_o and U are taken as 1.139 kg/m^2 and 2.7 m/s, from earlier studies (26) and meteorological data (27), respectively. Air dynamic viscosity was assumed to be 1.9065 x 10^{-5} kg/m.

However, there is another pressure difference—one between the classroom and the outside corridor (next to the door). From established building code standards (28), we can conclude that pressure differential P_{indoor} between the classroom and corridor will be 5–20 Pa, resulting in the net pressure gradient from window-to-door (i.e., main inlet to main outlet) to be

$$\triangle P_{total} = \triangle P_w + \triangle P_{indoor} \quad (7)$$

From the above assessments, the individual pressure gradients approximate to $\triangle P_w = 3.5$ and $\triangle P_{indoor} = 5$ Pa. In the simulations, windows were taken as pressure inlets with 0-gauge pressure, nostrils were taken as velocity inlets with volumetric flux at 15 L/min (21, 29–32) to replicate gentle steady breathing, and at the door, we imposed a pressure outlet condition with negative gauge pressure of $\triangle P_{total}$, i.e., −8.5 Pa. Wall boundary conditions were mimicked as a stationary wall with no slip condition.

Modeling impact of class size on SARS-CoV-2 exposure

The probability that at least one student in a classroom arrives infected with SARS-CoV-2 was estimated from the overall prevalence of the infection using Poisson statistics. This probability P was estimated as

$$P = 1 - e^{-nf} \quad (8)$$

where n is the number of students in the classroom and f is the fraction of infected individuals in the overall population. To estimate the expected number of exposed individuals in a school with N total students, the entire student population was broken into classes with i students each. The probability that at least one student in each class P_i was estimated using the above equation, and the expected number of students exposed to an infected individual was then calculated as NP_i.

Results

To study SARS-CoV-2 transmission and the impact of control measures in schools, we created a multistep mathematical model of viral transmission in indoor settings (Methods) occurring under the assumption of indoor aerosol spread of infectious virus (see Supplementary material S3 for justification of this assumption). First, we estimated the concentration of virions in the air over time in a room with an infected individual present using a differential equations model. This model assumes that infected individuals emit virions into the air at a constant rate into a room that is modeled as a well-mixed container (see Supplementary material S4 for details about this assumption). Emitted virions can be inactivated over time or filtered out *via* air exchanges. These viral concentration estimates were then used as an input to calculate the probability that uninfected individuals in the room will become infected with SARS-CoV-2.

Viral concentrations in a room with an infected individual present reach steady state quickly

Under this model of SARS-CoV-2 emission, the viral concentration in a room reaches a steady-state concentration after the infected individual has been present for a certain time. For a closed room without air exchange or filtration, this concentration C_{SS} depends on the emission rate α, viral inactivation rate δ, and the volume of the room V and is estimated as $C_{SS} = \alpha/(\delta V)$ (Methods). To understand the impact of evolutionary changes in viral load, we picked three variants of the virus whose viral loads have been reported in the literature to be widely different from one another (see Supplementary material S5 for details about viral loads for the ancestral strain and the Delta and Omicron variants). For a typical classroom size (20 x 20 x 10 feet), the steady-state concentration with an individual infected with the ancestral virus is approximately 4 virions per liter, which scales linearly for higher viral load SARS-CoV-2 strains (Figure 1). We found that this steady-state concentration is reached after an infected individual is present in a room for 1–2 hours, regardless of the rate at which the individual emits viral particles. Masking of the emitter decreases the rate at which infected individuals release virions, lowering the final steady-state concentration, but does not affect the time at which the steady state is reached (see Supplementary material S6 for details about parameter estimates for various interventions in this and subsequent sections). We further explore the effects of different types of masks on the steady-state viral concentration later in this section (Figure 6). After the infected individual leaves the room, the viral concentration returns to approximately zero over a

5-hour period in a closed room (Supplementary Figure S2). Of note, the observed fast viral accumulation kinetics along with the slow viral clearance is particularly concerning in situations where students frequently change classrooms, as lingering viral particles from a student no longer in the room would be capable of causing more infections. This kinetic behavior may thus lead to a higher risk of infection than we have directly modeled here.

Steady-state concentrations of virions are reduced by high-volume air filtration

Filtering the air in the room decreases the steady-state concentration of virions by increasing the rate at which infectious virions are eliminated from the room (Methods). For infected individuals with a low viral emission rate (e.g., infected with the ancestral SARS-CoV-2 virus), air filtration and masking of the infectious individual can reduce the steady-state concentration of virus in the room to less than one virion per liter of air (Figure 2). However, for SARS-CoV-2 variants and individuals with higher viral loads and therefore higher viral emission rates (e.g., with Omicron-like viral loads, represented here as the "medium" rate, or with Delta-like viral loads, represented here as the "high" emission rate), the steady-state viral concentration in the room might remain high even with high filtration efficiency and filtration rate (Figure 2). Notably, for schools using high efficiency filtration systems (e.g., high-efficiency particulate air or HEPA filters), increasing the rate of air exchange across the filter is important for minimizing transmission.

Steady-state concentrations of virions in the air are decreased by ionizers

Another strategy to lower the viral concentration is to use ionizers, which inactivate viral particles and remove them from the air (33). These devices produce small ions by the corona discharge principle, according to which negatively charged ions transfer their charge to suspended particles upon collision. These charged particles then agglutinate, becoming larger until they fall out of the air under the effect of gravity (34). Ionizers generating negatively charged ions have been shown to be efficient at removing bacteria, molds, and viruses from indoor air (35–37). The efficiency of particle removal is dependent on the emission rate of ions within an enclosed space, as well as room volume (38). Studies conducted with smoke particles in an enclosed room suggest a high efficiency of ionizers in removing particles from the air, that varies between 80 and 100% (34, 38, 39). Although older ionizer technologies generate ozone, which is an undesirable byproduct, newer ionizers do not have this potential liability associated with them (40).

As with the other control measures we simulated, we found that ionizers can lower viral concentrations in a typical classroom to below one virion per liter in situations where the infected individual is emitting viral particles at a relatively low rate (masked, infected with a low viral load strain) (Figure 3). However, if the individual is infected with a high viral load SARS-CoV-2 variant (e.g., Delta), the viral concentration in the room will be very high even when ionizers are being used (Figure 3).

Only a fraction of inhaled viruses is deposited in the nasopharynx

We used the viral concentration estimates calculated in the previous section, estimates of aerosolized particle deposition derived from computational fluid dynamics (CFD) modeling, and the minimum infectious dose of SARS-CoV-2 to estimate the probability that uninfected individuals in the room will become infected with SARS-CoV-2.

Infection of a new host requires the virus to be inhaled and deposited on the airway mucosa, where it can replicate. To study transmission dynamics in indoor settings with airborne SARS-CoV-2, we used a published computational fluid dynamics model of airflow in the nasopharynx to estimate the number of inhaled viral particles that are deposited in the airway mucosa (21). This computational model of airflow in the human nasopharynx estimates the probability that an inhaled virion will reach the airway mucosa, given the size of the liquid droplet in which it is suspended. We assumed individuals breathe in virions suspended in liquid droplets with the measured steady-state size distribution of expelled respiratory droplets (22). We used the computational fluid dynamics modeling results to compute the overall probability that an inhaled virion will hit the nasopharynx, marginalized over the empirical droplet size distribution [(Methods), Supplementary Table S1], and found that approximately 0.6% of virions that are inhaled during each breath are deposited in the mucosa.

Masks and air filtration reduce the expected number of virions transmitted to uninfected individuals

We used this nasopharyngeal deposition probability to estimate the number of virions that reach the airway mucosa per hour in an uninfected student in a classroom with a given concentration of SARS-CoV-2 in the air (Methods). For a classroom with an individual emitting virions at a low rate, interventions such as masking and air filtration can lower the transmission rate to an uninfected individual to <1 virion per hour, preventing transmission for short periods in the

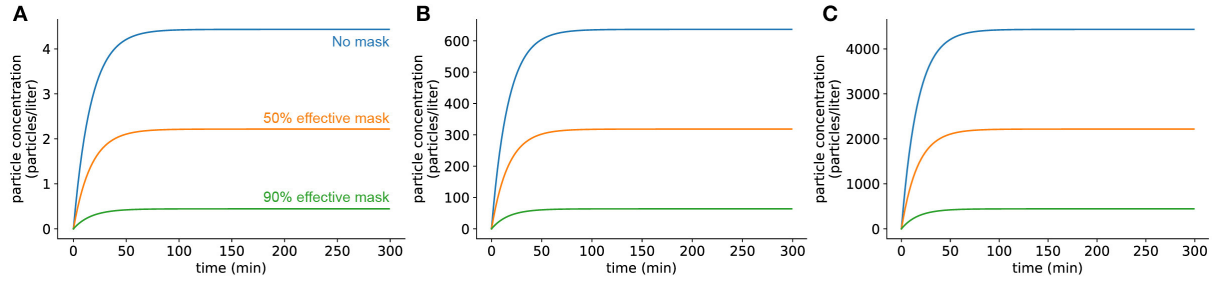

FIGURE 1
Viral concentrations in a room with an infected individual present reach steady state quickly. **(A)** Infected individual with a low viral load strain of virus (similar to the ancestral strain). **(B)** Individual infected with an intermediate viral load variant (similar to Omicron). **(C)** Individual infected with a high viral load variant (similar to Delta). Room dimensions are 10′ x 20′ x 20′. No air filtration or other mitigation methods were used. In all panels, the blue curve shows the concentration when the infected individual has no mask on, the orange curve shows the concentration when the infected individual has on a mask which filters out 50% of exhaled particles (typical cloth mask), and the green curve shows the concentration when the infected individual has on a mask which filters out 90% of exhaled particles (typical surgical mask).

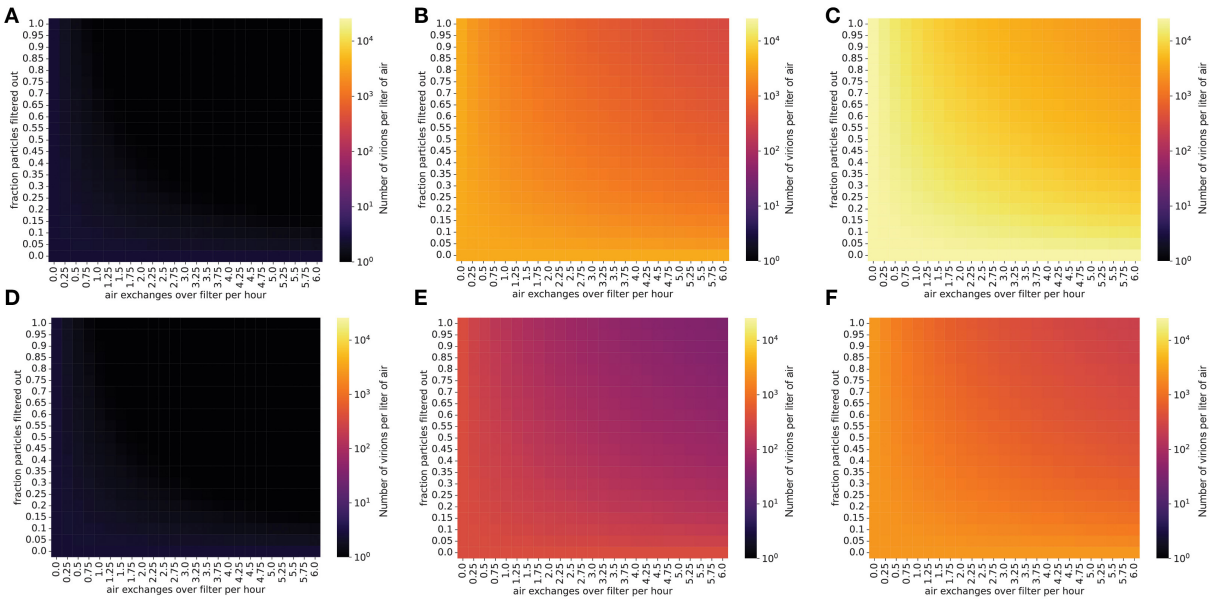

FIGURE 2
Steady-state concentrations of virions are strongly impacted by air exchange rate across the filter and by the fraction of particles removed when air is passed over the filter. Virion concentrations at steady state, in a room 10′ x 20′ x 20′. **(A–C)** Individual infected with a low viral load, **(A)** intermediate viral load, **(B)** or high viral load, **(C)** strain, no mask. **(D–F)** Individual infected with a low viral load, **(D)** intermediate viral load, **(E)** or high viral load, **(F)** strain, wearing a 90% effective mask. Typical air purification systems can achieve a filtration rate of approximately 5–6 exchanges/h (Supplementary material S6).

classroom (Figure 4). However, exposure over several hours or an entire school day may transmit enough virions to the nasopharynx to cause infection, so limiting contact and masking of uninfected students is still important for controlling viral spread in this situation. If the virus-emitting individual is infected with a high viral load variant (similar to Delta), the number of virions inhaled can increase to hundreds or thousands per hour, possibly causing infection even after only a short exposure period (Figure 4). In fact, while several hours are required for transmission of a low viral load (ancestral-like) variant in a classroom, an individual infected with a high viral load (Delta-like) variant can spread the virus within a matter of minutes (Figure 5). Thus, in this scenario, with multiple environmental control measures (masking and air filtration) in place, transmission can still occur over an 8-hour school day. Thus, in a future scenario where we are faced with a Delta-like variant with high viral loads, schools may have to rely on additional measures (e.g., rapid and widespread surveillance

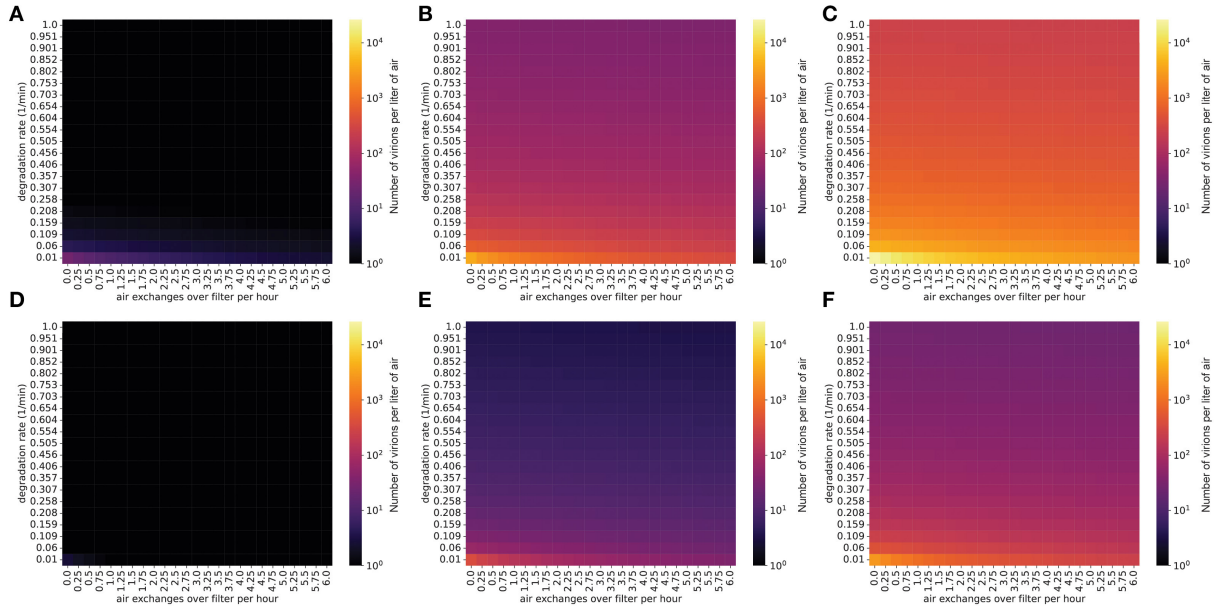

FIGURE 3
Steady-state concentrations are decreased by ionizers (which increase the particle degradation rate). Virion concentrations at steady state, in a room with the same dimensions as Figure 1. **(A–C)** Individual infected with a low viral load, **(A)** intermediate viral load, **(B)** or high viral load, **(C)** strain, no mask. **(D–F)** Individual infected with a low viral load, **(D)** intermediate viral load, **(E)** or high viral load, **(F)** strain, wearing a 90% effective mask. The degradation rate of airborne SARS-CoV-2 without the use of an ionizer is approximately 0.01/min.

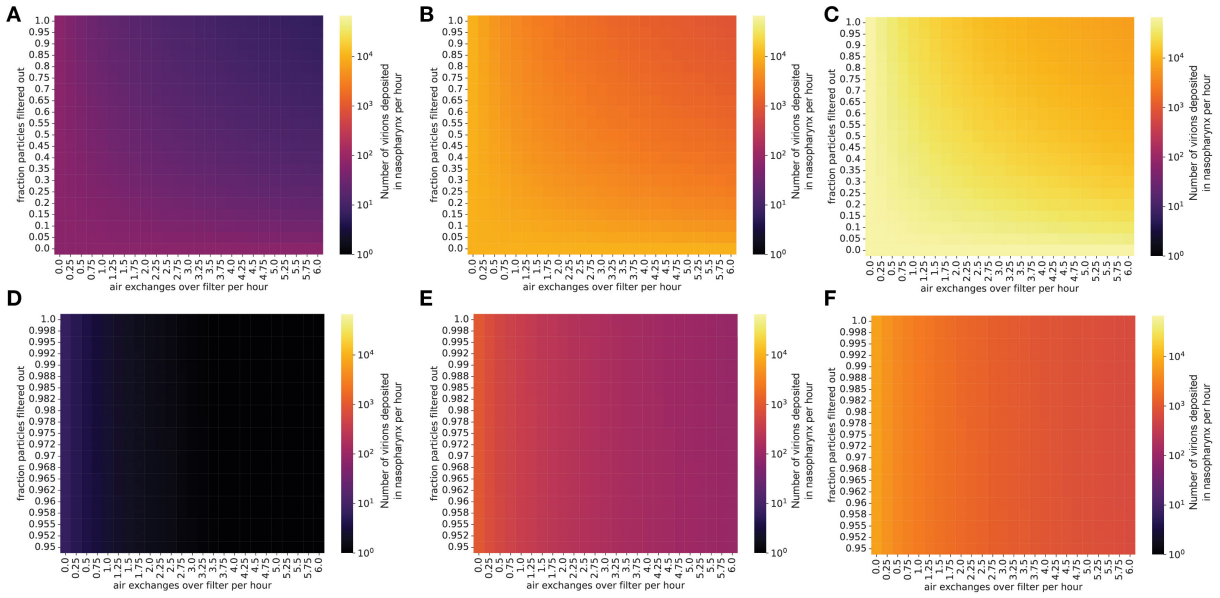

FIGURE 4
Even with masks and air filtration, a person exposed to a high viral load emitter will be exposed to thousands of virions per day. Virions inhaled by an uninfected individual per hour in the presence of an infected individual, in a room with the same dimensions as Figure 1. The probability that an inhaled virion hits nasopharynx was estimated at 0.6% (methods). **(A–C)** Individual infected with a low viral load, **(A)** intermediate viral load, **(B)** or high viral load, **(C)** strain, no mask. **(D–F)** Individual infected with a low viral load **(D)**, intermediate viral load **(E)**, or high viral load **(F)** strain, with the emitter wearing a 90% effective mask (one-way masking).

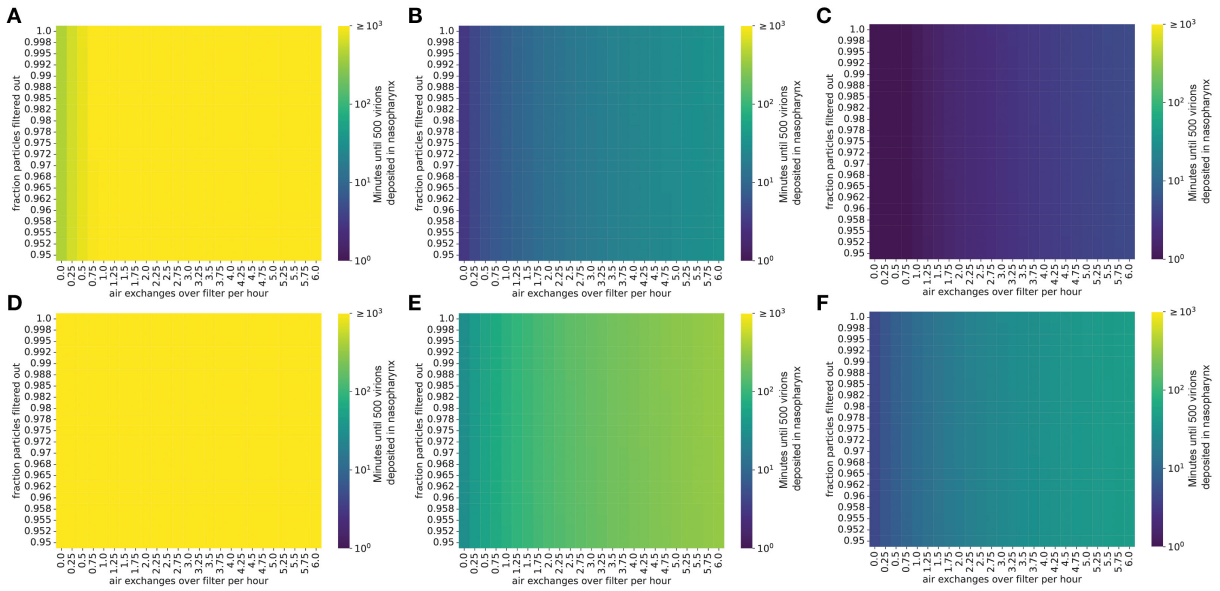

FIGURE 5
The presence of robust mitigation measures substantially increases the time to infection for low viral load strains. Plots show the time until an uninfected individual receives 500 virions in a room occupied by an infected individual. **(A–C)** Individual infected with a low viral load, **(A)** intermediate viral load, **(B)** or high viral load, **(C)** strain, no mask. **(D–F)** Individual infected with a low viral load, **(D)** intermediate viral load, **(E)** or high viral load, **(F)** strain, with the emitter wearing a 90% effective mask (one-way masking).

testing, targeted school closures) to limit in-school spread. These measures would need to supplement and not replace in-school mitigation measures in order to be effective.

Two-way masking can substantially reduce the number of virions transmitted

High-quality masks, used correctly, have been demonstrated to reduce infection risk even in high-risk settings (41–43). Therefore, such masks can provide an additional level of mitigation in the event that schools are faced with a high viral load (Delta-like) variant. Masks provide a double benefit, as they reduce transmission by filtering out virions emitted by infected individuals and by reducing the number of ambient virions inhaled by uninfected individuals. Masks that filter out >95% of virions increase the time to transmission by approximately 10-fold when worn on either the infected or uninfected individual [(one-way masking); Figure 6]. If both the infected and uninfected individuals are masked (two-way masking), less-effective masks (e.g., well-fitted surgical masks) can achieve the same level of protection against transmission. Combining universal N95 masking with excellent ventilation can increase the time to transmission of even high viral load strains to longer than a typical school day (Figure 6D), suggesting that layered mitigation strategies featuring well-fitted and high-quality masks are critical for the control of high viral load strains in the classroom.

In a well-ventilated room, risk is strongly dependent on seating position relative to the infected individual

Up to this point, we have considered the classroom to be a well-mixed container. This simple modeling approach allows us to identify settings where the risk of in-school transmission is high. The well-mixed container assumption is justified, particularly in settings with limited ventilation (see Supplementary material S4 for details). However, in some settings, the assumption may not hold, particularly in well-ventilated rooms, which are thought to have a low risk of transmission overall. To better understand the risk of transmission in a well-ventilated setting, we used CFD simulations of air transport inside a classroom. To simulate a best-case scenario for ventilation, we chose to model airflow behavior with the dimensions of a large auditorium-style classroom in a tropical setting, with high ceilings and several windows that are all open (Figures 7A–C). We placed a single infected individual (emitter) in the room and varied their position to understand the impact of the airflow in the room.

Figure 7D visually depicts the airflow mixing trends inside the room and the virion-bearing streamline patterns for emitters

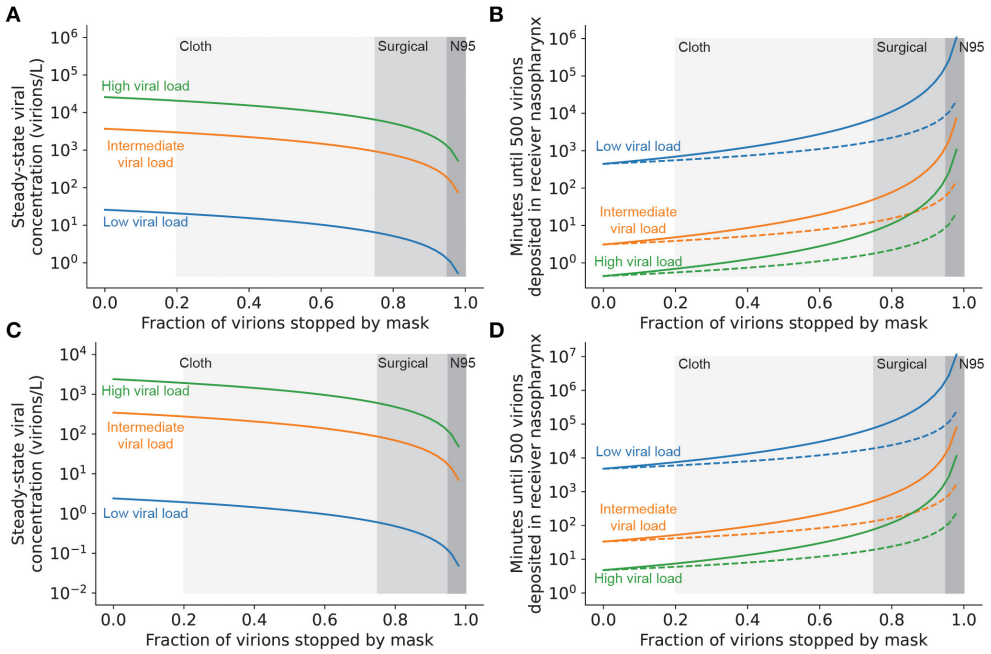

FIGURE 6
Masking both infected and uninfected individuals reduces the rate of viral transmission. **(A)** Steady-state airborne viral concentration in an unventilated classroom with a single infected individual wearing a mask with the filtration efficiency given on the x-axis. **(B)** Time until infection of uninfected individuals present in an unventilated classroom with a single infected individual wearing a mask with the filtration efficiency given on the x-axis. Uninfected individuals either are not wearing masks (one-way masking; dashed lines) or are wearing a mask with the same filtration efficiency as the infected individual (two-way masking; solid lines). **(C)** Steady-state airborne viral concentration in a well-ventilated classroom (6 complete air exchanges per hour) with a single infected individual wearing a mask with the filtration efficiency given on the x-axis. **(D)** Time until infection of uninfected individuals present in a well-ventilated classroom with a single infected individual wearing a mask with the filtration efficiency given on the x-axis. Uninfected individuals either are not wearing masks (one-way masking; dashed lines) or are wearing a mask with the same filtration efficiency as the infected individual (two-way masking; solid lines). In all panels, shaded regions denote typical filtration efficiencies for cloth, surgical, and N95 masks (Supplementary material S6) and curve colors denote viral load of the emitter.

located at different parts of the auditorium-style classroom. As the room is well-ventilated, the aerosolized virions emitted by the infected individual (Figure 7E) standing on the podium at the front of the room (with a door located proximally on the side), as well as those from the individual seated in the front row (Figure 7F), would escape through the door quite readily. The situation is, however, different if the infected individual were seated in the middle of the room (Figure 7G), and even worse if the infected individual were seated at the rear (Figure 7H). In these two situations, the infected individual would be efficiently spreading aerosolized pathogens, *via* exhaled respiratory ejecta, through the entire room. Thus, for a well-ventilated room (where the well-mixed container assumption cannot be expected to apply) total viral load in the room depends strongly on the position of the infected individual in the room. Additionally, local virion concentrations may be sufficiently high to enable efficient viral spread in the absence of other countermeasures (such as masking). The chaotic airflow patterns (invisible to the naked eye) underscore the unpredictable downside of infection risk in a closed setting (Figure 7H).

Thus, while it is possible to use model-based approaches to identify settings with a high risk of transmission, model-based approaches that rely on the well-mixed container assumption cannot definitively identify indoor settings with a low risk of transmission. This finding further underscores the need for multiple layers of intervention, and a robust ability to detect outbreaks before they spread.

Measures to reduce the likelihood of infected individuals being present in the classroom setting are crucial

Environmental control measures (masking, air filtration, and ionizers) can all have an impact on limiting transmission in the in-school setting. However, our work suggests that these measures—both individually and in concert—are all vulnerable to defeat by a sufficiently high burden of virion emission. Thus, reducing the probability of infected individuals being present in the classroom at all is crucial to limiting SARS-CoV-2 transmission in schools. To that end, three measures are critical for reducing the expected number of infected individuals in a classroom: testing, capacity limits, and targeted school

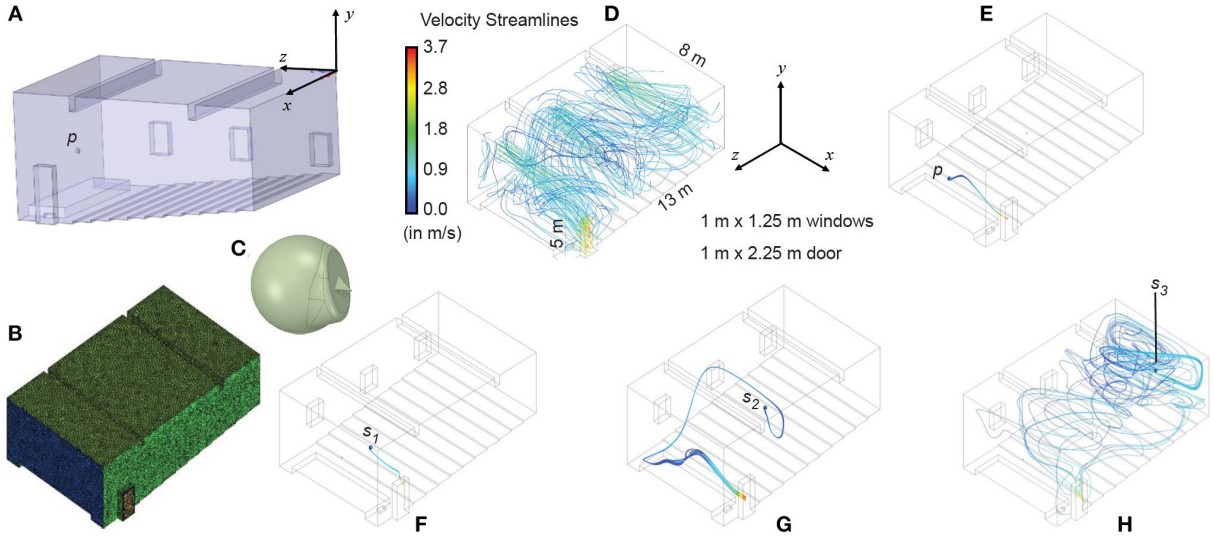

FIGURE 7
In a well-ventilated room, infection risk is strongly dependent on the location of the infected individual. **(A)** Digitized geometry of a classroom (based on direct measurements of an auditorium-style classroom in a tropical setting). The position of the instructor's head is marked by *p*. **(B)** Meshed space interior to the bounds of the classroom. **(C)** Typical head geometry for the emitter subtracted from the classroom mesh, with realistic nostril diameters. **(D)** Mixing of velocity streamlines in the classroom with the windows as the inlet and the door as the outlet. The panel includes the layout and plan dimensions of the ventilated classroom. **(E–H)** Flowlines of exhaled virions showing the impact of emitter location (blue dot: p represents the instructor's head location, s_{1-3} represent the students' head locations) on local concentrations of virions. Note that s_1 is in the front seat, s_2 is in the middle of the classroom, and s_3 is in the rear seat. Local concentrations are dependent on fluid dynamics within the classroom, suggesting that even if the average concentration of virions in a room is below the infectious threshold, individuals may become infected over time based on their location downstream of the emitter.

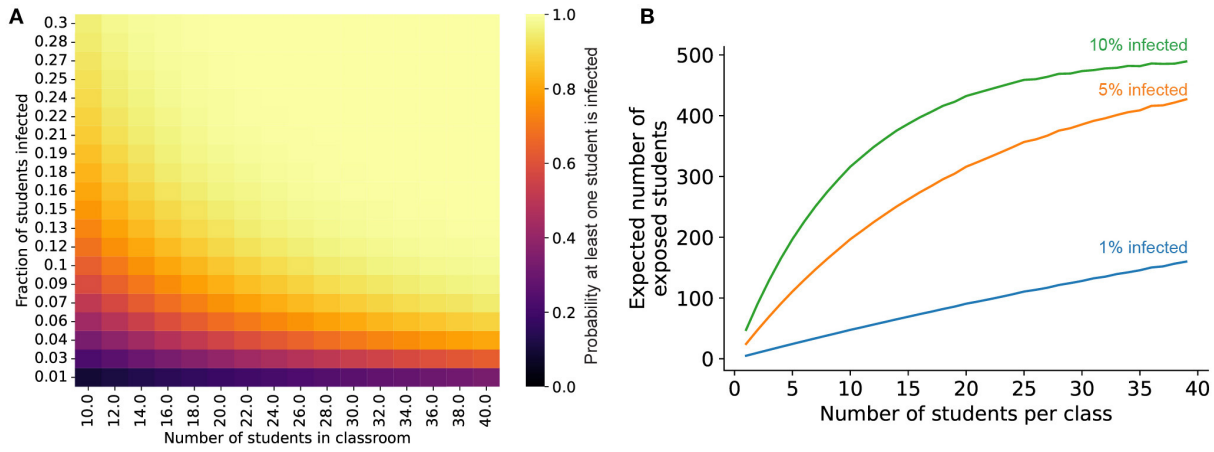

FIGURE 8
Reducing class sizes reduces the risk of infection in school settings. **(A)** Probability that at least one student in a classroom is infected, given values for the population-level infection prevalence (y-axis) and the number of students in the classroom (x-axis). **(B)** Expected number of students exposed to an infected individual in a 500-person school when the school is broken up into different size classes over the entire school day (see Methods for additional details), given different values for the initial overall SARS-CoV-2 infection prevalence in the student population (blue curve: 1% of students infected, orange curve: 5% infected, green curve: 10% infected).

closures. Regular screening tests, with infected individuals being identified and isolated before they enter the classroom, can reduce the number of expected infected individuals arriving at school each day. Reducing class sizes by running the school day in shifts or by offering a remote school option to students that prefer it can also reduce the expected number of infected individuals in schools (Figure 8). Podding, which limits students' exposure to others outside of their cohort, such as in

the lunchroom, can interrupt transmission chains to prevent spread throughout the school. Similarly, keeping schools closed for periods of time when local transmission is high would also have a proportional impact on reducing transmission. Notably, widespread vaccine coverage—which is essential to limit the mortality and morbidity burden of the ongoing COVID-19 pandemic—may not play a significant role in limiting transmission at present (see Supplementary material S8 for a summary of vaccinal efficacy against transmission).

Discussion

In this study, we have used mathematical modeling to demonstrate the strengths and limitations of a layered mitigation strategy in limiting in-school transmission while keeping schools open. We examined the impact of risk mitigation measures (masking, ionizers, ventilation, and filtration) on limiting spread within a classroom when an infected person is present. Our findings underscore the critical importance of layered mitigation strategies in limiting in-school transmission. With that said, all of the examined measures can be readily defeated by sufficiently high viral loads, a biological change that has already been observed during the pandemic (for example between the ancestral strain and the Delta variant). This is a crucial point: minimal effective measures for the disease as it is at present may have an increased risk of failure in the face of new variants of SARS-CoV-2. Our findings also indicate that the risk of transmission in schools may be hard to predict in certain settings (such as in the turbulent airflow patterns of a well-ventilated room). As a corollary, our work points to the central importance of relying on measures to limit the likelihood of having an infected person in the classroom: testing and isolation, limiting class sizes, and targeted closures when community transmission is high.

The ongoing COVID-19 pandemic shows no signs of permitting a return to pre-pandemic life, with high rates of transmission leading to rapid viral evolution. The course of the pandemic under these conditions is likely to be unpredictable, with the potential for catastrophic levels of mortality and morbidity should new variants of the virus emerge that have greater immune evasion potential or virulence. Thus, slowing viral evolution by limiting transmission is now a vital societal imperative. Reducing transmission and avoiding further COVID-19 waves is particularly important in light of the growing awareness of the possibility of long-term consequences of infection (long COVID), which will likely lead to serious human and economic costs over the coming years (44, 45).

There are many examples in human society where the routine operation of vital services provided by complex systems brings some measure of risk to those involved: road transportation, aviation, medical care, law enforcement, agriculture and power generation, to name a few. In each of these cases, risks are managed by using a systems approach, where multiple layers of different interventions are used to reduce the risk of overall failure (46). The premise is that accidents in complex systems occur through the accumulation of failures. This "Swiss Cheese model" (47) of risk mitigation is well-known in the epidemiological community, and a number of epidemiologists have advocated for its use from the beginning of this pandemic (48, 49). The strength of the Swiss Cheese model in risk management lies in building a system that is robust to human error. Our results suggest that multilayered, multimodal interventions are necessary to control SARS-CoV-2 spread in schools, particularly in the face of new, more transmissible variants. In the specific case of an evolving virus, the Swiss Cheese model also provides multiple orthogonal selection pressures, making escape more difficult for the virus. To keep schools open, designing guidelines to limit transmission based on the Swiss Cheese model, and then validating those guidelines to ensure robustness to epidemiological changes driven by viral evolution, will be critical.

In the school setting, the application of the Swiss Cheese model has been slow for a number of reasons: the risk of in-school transmission has been under-estimated or compared to the wrong outcome (health effects on children), and false dichotomies in strategic thinking have led to an inappropriate focus on some layers of the "Swiss Cheese" in preference to others (for example, arguing for unmasking because children are vaccinated, or arguing for eliminating testing and contact tracing because children are masked). At this point, there is clear evidence supporting the contention that SARS-CoV-2 transmission can occur in schools (11, 50). The public-health consequences of that transmission are not borne by children alone. In addition to the first-order effect of household transmission of school-acquired COVID-19, transmission in the school setting facilitates viral evolution. An evolving virus benefits from a narrow focus on individual measures—the more focused the selection pressure, the easier it is for the virus to escape it. The mistake of over-reliance on one layer of the Swiss Cheese Strategy (made with the vaccines) can easily be repeated with other measures (such as testing and contact tracing).

This work has several assumptions and key limitations. We have assumed for most of the work that the classroom is a well-mixed container, and then demonstrated that the failure of this assumption may lead to higher infection risk (Figure 7). We also assumed that children are equally susceptible and infectious as adults (see Supplementary material S1 for an in-depth discussion of this assumption). We also assumed perfect compliance with mask-wearing, which is not likely to be true in practice (51, 52). We also have not considered the effect of vaccination on transmission or risk of infection—primarily because the role of vaccines in limiting SARS-CoV-2 infection (and transmission) has now been demonstrated to be highly time-sensitive and vulnerable to immune evasion (see Supplementary material S8 for an in-depth justification of

this assumption). Finally, in this study we relied solely on computational modeling to explore the impacts of different interventions on indoor COVID-19 transmission. Our work thus takes a first-principles deductive approach and relies on the underlying mechanistic framework for its validity. This approach is in contrast to the use of direct empirical validation, which would require a lengthy prospective randomized control trial, rendering the circumstances of the work moot over a period of months or years. Our results have immediate actionable implications for public health policy—we note that rigorous modeling studies have been used previously to guide policy decisions around the design of interventions for limiting SARS-CoV-2 transmission, in particular in China (53–55). Additionally, the simplicity and interpretability of our environmental transmission model make it easier to explain our results to not only public health policy makers but also frontline staff (e.g., teachers and administrators) and members of the public that would be directly involved in implementing our proposed interventions. The take home message from this work can be succinctly explained thus: using multiple layers of mitigation can greatly reduce the risk of transmission in a school setting, with the limitation that viral variants with very high viral loads may not be tractable to this approach. Effectively communicating the reasoning behind the policy recommendations will likely improve adherence.

There are a number of very thoughtful modeling analyses on this topic that have been published throughout the course of this pandemic. Several other groups have used model-based analyses to demonstrate that in-school transmission of SARS-CoV-2 is likely to be significant (12, 13, 56). The point that reopening schools without robust COVID-19 mitigation could lead to an acceleration of the pandemic has been made in several modeling studies (57–59). At the same time, a number of groups have published models focused on a limited set of infection-control measures, to show how schools can be reopened without risking in-school transmission [for example by using portable air purifiers (60), limiting class sizes (61), or mandating vaccination (62, 63)]. Our work adds to the discussion by pointing out the need to take evolutionary-driven epidemiological changes (for example due to viral load from one variant to the next) into account. In his book *The Black Swan* (now a classic in the risk-management community), author Nasim Nicholas Taleb argues that the key to risk management lies not so much in predicting the worst thing that could happen, but in making plans that are robust to that outcome.

Conclusion

Our modeling demonstrates that a layered mitigation strategy, implemented properly, can curtail viral transmission under many circumstances. With that said, there are ways to implement infection-control measures that are ineffective, and measures that are effective in the presence of one viral variant can be readily rendered ineffective in the presence of another. Because many of the interventions have a non-linear effect on risk mitigation, cutting corners on risk mitigation steps can degrade their utility very quickly, turning them into "hygiene theater". For example, we found that two-way masking with N95 masks increases the time until SARS-CoV-2 transmission by multiple orders of magnitude, as compared to one-way masking with cloth or surgical masks (Figure 6). Additionally, it is crucial for schools to have controls in place to ensure that measures taken for mitigation are working as intended. For example, air quality can be monitored using carbon dioxide monitors, and mandatory (as opposed to opt-in) testing can be used to monitor the functional outcomes of in-school mitigation. Mitigation strategies should be pressure-tested using simple mathematical modeling approaches such as the one described in this paper. Thresholds for the acceptable performance of mitigation measures (for example, air filters or ionizers) should be updated periodically to reflect changes in viral epidemiology. Thus, only by iterative optimization of control measures can we expect to have effective suppression of in-school transmission of SARS-CoV-2. Taking a risk-management mindset to the problem of developing layered measures for infection control in the school setting is crucial at this stage. Unfortunately, as the Centers for Disease Control continues to ease guidelines designed to prevent indoor COVID-19 transmission, schools in the US may find it difficult to establish such measures or keep them in place. Nevertheless, implementing such approaches to ensure robustness in the face of viral evolution may allow us to escape the false dichotomy of keeping schools open vs. bringing the pandemic to an end.

Data availability statement

The datasets and simulation code used in this study can be found at https://github.com/dvanegeren/covid-indoor-transmission.

Author contributions

DV and AC designed the study, with additional help conceptualizing the methods by SB, MS, and DL. Implementation, analysis, and visualization of the viral transmission modelling was performed by DV and DL, with supervision from AC. The computational fluid dynamics simulations were performed and visualized by AM, DG, AA, SM, and BM under the supervision of SB. The original draft of the manuscript was written by DV, SB, and AC. RN, DJ-M, LW, and NH provided additional supervision and editing. All authors contributed to the article and approved the submitted version.

Funding

This material is based upon work partially supported by the National Science Foundation (NSF) RAPID Grant 2028069 for COVID-19 research, with SB as the Principal Investigator. Any opinions, findings, and conclusions or recommendations expressed here are, however, those of the author and do not necessarily reflect NSF's views. Fractal Therapeutics provided salary support for author MS.

Acknowledgments

We thank Dr. Ed Parsons and Michael Walters for helpful discussions and feedback.

Conflict of interest

Authors AC and MS are employed by Fractal Therapeutics. Author RN is employed by Halozyme Therapeutics. Authors AC, MS, RN, DV, and DJ-M are shareholders in Fractal Therapeutics.

The remaining authors declare that the research was conducted in the absence of any commercial or financial relationships that could be construed as a potential conflict of interest.

Publisher's note

All claims expressed in this article are solely those of the authors and do not necessarily represent those of their affiliated organizations, or those of the publisher, the editors and the reviewers. Any product that may be evaluated in this article, or claim that may be made by its manufacturer, is not guaranteed or endorsed by the publisher.

Supplementary material

The Supplementary Material for this article can be found online at: https://www.frontiersin.org/articles/10.3389/fpubh.2022.941773/full#supplementary-material

References

1. Van Egeren D, Novokhodko A, Stoddard M, Tran U, Zetter B, Rogers M, et al. Risk of rapid evolutionary escape from biomedical interventions targeting SARS-CoV-2 spike protein. *PLoS ONE.* (2021) 16:e0250780. doi: 10.1371/journal.pone.0250780

2. Hirabara SM, Serdan TDA, Gorjao R, Masi LN, Pithon-Curi TC, Covas DT, et al. SARS-CoV-2 variants: differences and potential of immune evasion. *Front Cell Infect Microbiol.* (2021) 11:781429. doi: 10.3389/fcimb.2021.781429

3. Liu Y, Rocklöv J. The reproductive number of the delta variant of SARS-CoV-2 is far higher compared to the ancestral SARS-CoV-2 virus. *J Travel Med.* (2021) 28:taab124. doi: 10.1093/jtm/taab124

4. Alimohamadi Y, Taghdir M, Sepandi M. Estimate of the basic reproduction number for COVID-19: a systematic review and meta-analysis. *J Prev Med Public Health.* (2020) 53:151–7. doi: 10.3961/jpmph.20.076

5. Sanche S, Lin YT, Xu C, Romero-Severson E, Hengartner N, Ke R. High contagiousness and rapid spread of severe acute respiratory syndrome coronavirus 2. *Emerg Infect Dis.* (2020) 26:1470–7. doi: 10.3201/eid2607.200282

6. Grant R, Charmet T, Schaeffer L, Galmiche S, Madec Y, Platen CV, et al. Impact of SARS-CoV-2 delta variant on incubation, transmission settings and vaccine effectiveness: results from a nationwide case-control study in France. *Lancet Reg Health Europe.* (2022) 13:100278. doi: 10.1016/j.lanepe.2021.100278

7. Lauer SA, Grantz KH Bi Q, Jones FK, Zheng Q, Meredith HR, Azman AS, et al. The incubation period of coronavirus disease 2019 (COVID-19) from publicly reported confirmed cases: estimation and application. *Ann Int Med.* (2020) 172:577–82. doi: 10.7326/M20-0504

8. Jansen L, Tegomoh B, Lange K, Showalter K, Figliomeni J, Abdalhamid B, et al. Investigation of a SARS-CoV-2 B.1.1.529 (Omicron) variant Cluster—Nebraska, November–December 2021. *MMWR Morb Mortal Wkly Rep.* (2021) 70:1782–4. doi: 10.15585/mmwr.mm705152e3

9. Statista Research Department. Share of U.S. family households with children, by type 1970–2020. In: *Statista.* (2021). Available online at: https://www.statista.com/statistics/242074/percentages-of-us-family-households-with-children-by-type/ (accessed March 14, 2022).

10. US Census Bureau. School enrollment in the United States: October 2020—detailed tables. In: *Census.gov.* (2021). Available online at: https://www.census.gov/data/tables/2020/demo/school-enrollment/2020-cps.html (accessed March 14, 2022).

11. White LF, Murray EJ, Chakravarty A. The role of schools in driving SARS-CoV-2 transmission: not just an open-and-shut case. *Cell Rep. Med.* (2022) 3:100556. doi: 10.31219/osf.io/2eh5m

12. Chernozhukov V, Kasahara H, Schrimpf P. The association of opening K—12 schools with the spread of COVID-19 in the United States: county-level panel data analysis. *Proc Nat Acad Sci.* (2021) 118:e2103420118. doi: 10.1073/pnas.2103420118

13. Lessler J, Grabowski MK, Grantz KH, Badillo-Goicoechea E, Metcalf CJE, Lupton-Smith C, et al. Household COVID-19 risk and in-person schooling. *Science.* (2021) 372:1092–7. doi: 10.1126/science.abh2939

14. Stein-Zamir C, Abramson N, Shoob H, Libal E, Bitan M, Cardash T, et al. large COVID-19 outbreak in a high school 10 days after schools' reopening, Israel, May 2020. *Euro Surveill.* (2020) 25:2001352. doi: 10.2807/1560-7917.ES.2020.25.29.2001352

15. Torres JP, Piñera C, De La Maza V, Lagomarcino AJ, Simian D, Torres B, et al. Severe acute respiratory syndrome coronavirus 2 antibody prevalence in blood in a large school community subject to a coronavirus disease 2019 outbreak: a cross-sectional study. *Clin Infect Dis.* (2021) 73:e458–65. doi: 10.1093/cid/ciaa955

16. Gold JAW, Gettings JR, Kimball A, Franklin R, Rivera G, Morris E, et al. Clusters of SARS-CoV-2 infection among elementary school educators and students in one School District—Georgia, December 2020–January 2021. *MMWR Morb Mortal Wkly Rep.* (2021) 70:289–92. doi: 10.15585/mmwr.mm7008e4

17. Fontanet A, Tondeur L, Grant R, Temmam S, Madec Y, Bigot T, et al. SARS-CoV-2 infection in schools in a northern French city: a retrospective serological cohort study in an area of high transmission, France, January–April 2020. *Eurosurveillance.* (2021) 26:2001695. doi: 10.2807/1560-7917.ES.2021.26.15.2001695

18. Crowe J, Schnaubelt AT, SchmidtBonne S, Angell K, Bai J, Eske T, et al. Assessment of a program for SARS-CoV-2 screening and environmental monitoring in an urban public school district. *JAMA Network Open.* (2021) 4:e2126447. doi: 10.1001/jamanetworkopen.2021.26447

19. Science and Technology Directorate. Estimated airborne decay of SARS-CoV-2. In: *US Department of Homeland Security.* (2022). Available online at: https://www.dhs.gov/science-and-technology/sars-airborne-calculator (accessed March 14, 2022).

20. Santarpia JL, Rivera DN, Herrera VL, Morwitzer MJ, Creager HM, Santarpia GW, et al. Aerosol and surface contamination of SARS-CoV-2 observed in quarantine and isolation care. *Sci Rep.* (2020) 10:12732. doi: 10.1038/s41598-020-69286-3

21. Basu S. Computational characterization of inhaled droplet transport to the nasopharynx. *Sci Rep.* (2021) 11:6652. doi: 10.1038/s41598-021-85765-7

22. Xie X, Li Y, Sun H, Liu L. Exhaled droplets due to talking and coughing. *J Royal Soc Interface.* (2009) 6:S703–714. doi: 10.1098/rsif.2009.0388.focus

23. Basu S, Witten N, Kimbell JS. Influence of localized mesh refinement on numerical simulations of post-surgical sinonasal airflow. *J Aerosol Med Pulmon Drug Deliv.* (2017) 30:A—14.

24. Kahsay MT, Bitsuamlak GT, Tariku F. CFD simulation of external CHTC on a high-rise building with and without façade appurtenances. *Build Environ.* (2019) 165:106350. doi: 10.1016/j.buildenv.2019.106350

25. Li Y. Role of Multi-Zone Models in Indoor Air Flow and Air Quality Analyses. *Indoor Environ.* (1993) 2:149–63. doi: 10.1177/1420326X9300200304

26. Rao KR, Balkundi HV. Study of variation in upper air density over India. *Def Sci J.* (1980) 30:31–44. doi: 10.14429/dsj.30.6411

27. India Meteorological Department. *Climate of West Bengal.* (2008). Available online at: https://imdpune.gov.in/library/public/Climate%20of%20WestBengal.pdf

28. International Organization for Standardization. *Cleanrooms and Associated Controlled Environments—Part 4: Design, Construction, and Start-up*. Geneva: International Organization for Standardization (2001).

29. Basu S, Holbrook LT, Kudlaty K, Fasanmade O, Wu J, Burke A, et al. Numerical evaluation of spray position for improved nasal drug delivery. *Sci Rep.* (2020) 10:10568. doi: 10.1038/s41598-020-66716-0

30. Basu S, Frank-Ito DO, Kimbell JS. On computational fluid dynamics models for sinonasal drug transport: relevance of nozzle subtraction and nasal vestibular dilation. *Int J Numer Method Biomed Eng.* (2018) 34:e2946. doi: 10.1002/cnm.2946

31. Farzal Z, Basu S, Burke A, Fasanmade OO, Lopez EM, Bennett WD, et al. Comparative study of simulated nebulized and spray particle deposition in chronic rhinosinusitis patients. *Int Forum Allergy Rhinol.* (2019) 9:746–58. doi: 10.1002/alr.22324

32. Brandon BM, Stepp WH, Basu S, Kimbell JS, Senior BA, Shockley WW, et al. Nasal airflow changes with bioabsorbable implant, butterfly, and spreader grafts. *Laryngoscope.* (2020) 130:E817–23. doi: 10.1002/lary.28691

33. Jiang S-Y, Ma A, Ramachandran S. Negative air ions and their effects on human health and air quality improvement. *Int J Mol Sci.* (2018) 19:2966. doi: 10.3390/ijms19102966

34. Uk Lee B, Yermakov M, Grinshpun SA. Removal of fine and ultrafine particles from indoor air environments by the unipolar ion emission. *Atmos Environ.* (2004) 38:4815–23. doi: 10.1016/j.atmosenv.2004.06.010

35. Hyun J, Lee S-G, Hwang J. Application of corona discharge-generated air ions for filtration of aerosolized virus and inactivation of filtered virus. *J Aerosol Sci.* (2017) 107:31–40. doi: 10.1016/j.jaerosci.2017.02.004

36. Wang C, Lu S, Zhang Z. Inactivation of airborne bacteria using different UV sources: performance modeling, energy utilization, and endotoxin degradation. *Sci Total Environ.* (2019) 655:787–95. doi: 10.1016/j.scitotenv.2018.11.266

37. Hagbom M, Nordgren J, Nybom R, Hedlund K-O, Wigzell H, Svensson L. Ionizing air affects influenza virus infectivity and prevents airborne-transmission. *Sci Rep.* (2015) 5:11431. doi: 10.1038/srep11431

38. Sawant VS, Meena GS, Jadhav DB. Effect of negative air ions on fog and smoke. *Aerosol Air Qual Res.* (2012) 12:1007–15. doi: 10.4209/aaqr.2011.11.0214

39. Grinshpun SA, Mainelis G, Trunov M, Adhikari A, Reponen T, Willeke K. Evaluation of ionic air purifiers for reducing aerosol exposure in confined indoor spaces. *Indoor Air.* (2005) 15:235–45. doi: 10.1111/j.1600-0668.2005.00364.x

40. Sung J-H, Kim M, Kim Y-J, Han B, Hong K-J, Kim H-J. Ultrafine particle cleaning performance of an ion spray electrostatic air cleaner emitting zero ozone with diffusion charging by carbon fiber. *Build Environ.* (2019) 166:106422. doi: 10.1016/j.buildenv.2019.106422

41. Wang X, Ferro EG, Zhou G, Hashimoto D, Bhatt DL. Association between universal masking in a health care system and SARS-CoV-2 positivity among health care workers. *J Am Med Assoc.* (2020) 324:703–4. doi: 10.1001/jama.2020.12897

42. Jehn M, McCullough JM, Dale AP, Gue M, Eller B, Cullen T, et al. Association between K—12 school mask policies and school-associated COVID-19 outbreaks—Maricopa and Pima Counties, Arizona, July–August 2021. *MMWR Morb Mortal Wkly Rep.* (2021) 70:1372–3. doi: 10.15585/mmwr.mm7039e1

43. CDC. Science brief: community use of masks to control the spread of SARS-CoV-2. In: *Centers for Disease Control and Prevention.* (2021). Available online at: https://www.cdc.gov/coronavirus/2019-ncov/science/science-briefs/masking-science-sars-cov2.html (accessed March 14, 2022).

44. Al-Aly Z, Bowe B, Xie Y. Long COVID after breakthrough SARS-CoV-2 infection. *Nat Med.* (2022) 28:1461–7. doi: 10.1038/s41591-022-01840-0

45. Robertson MM, Qasmieh SA, Kulkarni SG, Teasdale CA, Jones H, McNairy M, Borrell LN, Nash D. The epidemiology of long COVID in US adults two years after the start of the US SARS-CoV-2 pandemic. *medRxiv [preprint].* (2022). doi: 10.1101/2022.09.12.22279862

46. Reason J. Human error: models and management. *BMJ.* (2000) 320:768–70. doi: 10.1136/bmj.320.7237.768

47. Reason J. The contribution of latent human failures to the breakdown of complex systems. *Philos Trans Royal Soc Lond B Biol Sci.* (1990) 327:475–84: doi: 10.1098/rstb.1990.0090

48. Noh JY, Song JY, Yoon JG, Seong H, Cheong HJ, Kim WJ. Safe hospital preparedness in the era of COVID-19: the Swiss cheese model. *Int J Infect Dis.* (2020) 98:294–6. doi: 10.1016/j.ijid.2020.06.094

49. Roberts S. The Swiss cheese model of pandemic defense. In: *The New York Times.* (2020). Available online at: https://www.nytimes.com/2020/12/05/health/coronavirus-swiss-cheese-infection-mackay.html (accessed March 14, 2022).

50. Hyde Z. COVID-19, children and schools: overlooked and at risk. *Med J Aust.* (2020) 213:444–6.e1. doi: 10.5694/mja2.50823

51. Fischer CB, Adrien N, Silguero JJ, Hopper JJ, Chowdhury AI, Werler MM. Mask adherence and rate of COVID-19 across the United States. *PLoS ONE.* (2021) 16:e0249891. doi: 10.1371/journal.pone.0249891

52. Margraf J, Brailovskaia J, Schneider S. Adherence to behavioral Covid-19 mitigation measures strongly predicts mortality. *PLoS ONE.* (2021) 16:e0249392. doi: 10.1371/journal.pone.0249392

53. Zhang R, Wang Y, Lv Z, Pei S. Evaluating the impact of stay-at-home and quarantine measures on COVID-19 spread. *BMC Infect Dis.* (2022) 22:648. doi: 10.1186/s12879-022-07636-4

54. Qian Y, Cao S, Zhao L, Yan Y, Huang J. Policy choices for Shanghai responding to challenges of Omicron. *Front Public Health.* (2022) 10:927387. doi: 10.3389/fpubh.2022.927387

55. Zhou W, Bai Y, Tang S. The effectiveness of various control strategies: an insight from a comparison modelling study. *J Theor Biol.* (2022) 549:111205. doi: 10.1016/j.jtbi.2022.111205

56. Buja A, Zabeo F, Cristofori V, Paganini M, Baldovin T, Fusinato R, et al. Opening schools and trends in SARS-CoV-2 transmission in European countries. *Int J Public Health.* (2021) 66:1604076. doi: 10.3389/ijph.2021.1604076

57. Gurdasani D, Alwan NA, Greenhalgh T, Hyde Z, Johnson L, McKee M, et al. School reopening without robust COVID-19 mitigation risks accelerating the pandemic. *Lancet.* (2021) 397:1177–8. doi: 10.1016/S0140-6736(21)00622-X

58. Zhang Y, Johnson K, Yu Z, Fujimoto AB, Lich KH, Ivy J, Keskinocak P, Mayorga M, Swann JL. COVID-19 projections for K12 schools in fall 2021: significant transmission without interventions. *MedRxiv [preprint].* (2021). doi: 10.1101/2021.08.10.21261726

59. Panovska-Griffiths J, Kerr CC, Stuart RM, Mistry D, Klein DJ, Viner RM, et al. Determining the optimal strategy for reopening schools, the impact of test and trace interventions, and the risk of occurrence of a second COVID-19 epidemic wave in the UK: a modelling study. *Lancet Child Adolesc Health.* (2020) 4:817–27. doi: 10.1016/S2352-4642(20)30250-9

60. Narayanan SR, Yang S. Airborne transmission of virus-laden aerosols inside a music classroom: effects of portable purifiers and aerosol injection rates. *Phys Fluids.* (2021) 33:033307. doi: 10.1063/5.0042474

61. Baxter A, Oruc BE, Keskinocak P, Asplund J, Serban N. evaluating scenarios for school reopening under COVID19. (2020) *MedRxiv [preprint].* doi: 10.1101/2020.07.22.20160036

62. Panovska-Griffiths J, Stuart RM, Kerr CC, Rosenfield K, Mistry D, Waites W, Klein DJ, Bonell C, Viner RM. Modelling the impact of reopening schools in the UK in early 2021 in the presence of the alpha variant and with roll-out of vaccination against SARS-CoV-2. *J Math Anal Appl.* (2022) 126050. doi: 10.1016/j.jmaa.2022.126050

63. Head JR, Andrejko KL, Remais JV. Model-based assessment of SARS-CoV-2 Delta variant transmission dynamics within partially vaccinated K-12 school populations. *Lancet Reg Health Am.* (2022) 5:100133. doi: 10.1016/j.lana.2021.100133